

Self-starting all-fiber PM Er:laser mode locked by a biased nonlinear amplifying loop mirror

Ke Yin(殷科)[1,3], Yi-Ming Li(李仪茗)[2], Yan-Bin Wang(王彦斌)[4], Xin Zheng(郑鑫)[1], Tian Jiang(江天)[2]
Citation: Chin. Phys. B . 2019, 28(12): 124203 . **doi:** 10.1088/1674-1056/ab4d42
Journal homepage: http://cpb.iphy.ac.cn; http://iopscience.iop.org/cpb

What follows is a list of articles you may be interested in

Novel single-transverse-mode control of VCSELs with dielectric mode filter

Lei Xiang(向磊), Xing Zhang(张星), Jian-Wei Zhang(张建伟), You-Wen Huang(黄佑文), Yong-Qiang Ning(宁永强), Li-Jun Wang(王立军)
Chin. Phys. B . 2018, 27(7): 074210 . **doi:** 10.1088/1674-1056/27/7/074210

Stable single-mode operation of 894.6 nm VCSEL at high temperatures for Cs atomic sensing

Lei Xiang(向磊), Xing Zhang(张星), Jian-Wei Zhang(张建伟), Yong-Qiang Ning(宁永强), Werner Hofmann, Li-Jun Wang(王立军)
Chin. Phys. B . 2017, 26(7): 074209 . **doi:** 10.1088/1674-1056/26/7/074209

Frequency-stabilized Yb:fiber comb with a tapered single-mode fiber

Yang Xie(谢阳), Hai-Nian Han(韩海年), Long Zhang(张龙), Zi-Jiao Yu(于子蛟), Zheng Zhu(朱政), Lei Hou(侯磊), Li-Hui Pang(庞利辉), Zhi-Yi Wei(魏志义)
Chin. Phys. B . 2016, 25(4): 044208 . **doi:** 10.1088/1674-1056/25/4/044208

Experimental demonstration of single-mode fiber coupling using adaptive fiber coupler

Luo Wen, Geng Chao, Wu Yun-Yun, Tan Yi, Luo Qi, Liu Hong-Mei, Li Xin-Yang
Chin. Phys. B . 2014, 23(1): 014207 . **doi:** 10.1088/1674-1056/23/1/014207

Spontaneous emission of two quantum dots in a single-mode cavity

Qiu Liu, Zhang Ke, Li Zhi-Yuan
Chin. Phys. B . 2013, 22(9): 094207 . **doi:** 10.1088/1674-1056/22/9/094207

Self-starting all-fiber PM Er:laser mode locked by a biased nonlinear amplifying loop mirror*

Ke Yin(殷科)[1,3], Yi-Ming Li(李仪茗)[2], Yan-Bin Wang(王彦斌)[4], Xin Zheng(郑鑫)[1], and Tian Jiang(江天)[2,†]

[1] *National Innovation Institute of Defense Technology, Academy of Military Sciences PLA China, Beijing* 100071, *China*
[2] *College of Advanced Interdisciplinary Studies, National University of Defense Technology, Changsha* 410073, *China*
[3] *State Key Laboratory of High Performance Computing, College of Computer, National University of Defense Technology, Changsha* 410073, *China*
[4] *Luoyang Electronic Equipment Test Center of China, Luoyang* 471003, *China*

(Received 11 July 2019; revised manuscript received 3 September 2019; published online 22 November 2019)

A compact all-fiber polarization-maintaining Er:laser using a nonlinear amplifying loop mirror is reported. Fundamental single-pulse mode-locking operation can always self start, with a cavity round-trip decreased from ∼ 4.7 m to ∼ 1.7 m. When the pulse repetition rate is 121.0328 MHz, output pulse is measured to have a center wavelength/3-dB spectral bandwidth/radio frequency signal to noise ratio (SNR)/pulse width of 1571.65 nm/18.70 nm/80 dB/477 fs, respectively. Besides, three states including the exponential growth, damping state, and steady state are investigated through the build-up process both experimentally and numerically. Excellent stability of this compact Er:laser is further evaluated, demonstrating that it can be an easy-fabrication maintenance-free ultrafast candidate for the scientific area of this kind.

Keywords: ultrafast fiber laser, single-mode, polarization-maintaining Er:laser

PACS: 42.55.Wd, 42.60.Fc, 42.65.Re **DOI:** 10.1088/1674-1056/ab4d42

1. Introduction

Ultrafast mode-locked fiber lasers[1] which deliver pulses of extremely short duration (specifically, on the order of ps or fs) have proved to be powerful tools in many crucial scientific applications such as nonlinear optics,[2–4] precision metrology,[5,6] ultrafine material processing,[7] *etc*. To realize mode lock, thousands or tens of thousands of longitudinal modes must be forced to lock together by either real or equivalent saturable absorbers.[8–13] Compared with real saturable absorbers,[14–21] equivalent saturable absorbers based on the intra-cavity nonlinear effect highlight their advantages such as high damage threshold, ultrafast recovery time, and cost-effectiveness.

There are three most common equivalent saturable absorbers in mode-locked fiber lasers, namely nonlinear polarization evolution (NPE),[22–27] nonlinear loop mirror (NOLM),[28,29] and nonlinear amplifying loop mirror (NALM).[30,31] All of them could provide sub-100-fs laser pulse output from standard single-mode fibers.[32] However, NPE relies on the polarization rotation in fiber and is highly sensitive to environmental perturbations. Consequently, it is not deployable outside the laboratory. Both NOLM and NALM could be easily designed with polarization-maintaining (PM) fibers, and therefore this problem could be settled.[29] But original NOLM and NALM are hard to initiate mode lock because of limited peak power sensitivity. When incorporating with a nonreciprocal phase shifter properly, the nonlinear transmission of loop mirror could be shifted into the peak power sensitive region.[33] As a result, self-starting operations could be realized.

In 2016, a PM NALM mode-locked Er:fiber laser was demonstrated with unprecedented excellent stability against accelerations >10 g in a rocket launching process.[34] Despite that, in this laser a polarizing beam splitter and two wave-plates were adopted to tune intra-cavity nonreciprocal phase which needed carefully adjusting. In comparison, the adoption of all-fiber components made the laser fabrication process much easier, and greatly enhanced the laser stability and eliminated the uncertainty during adjustments. In 2017, an all-fiber PM NALM mode-locked Er:fiber laser was first put forward.[35] Although fully self-starting mode-locking operation was realized with a fundamental repetition rate of 48.8 MHz–64.7 MHz, the onset was in a multiple-pulse regime. Therefore, a stable single pulse operation could be obtained only by reducing the pump power to a lower value. Similar self-starting with multiple-pulse regime was also founded in a recent all-fiber PM Yb:laser mode locked by a biased NALM.[36]

In this paper, an all-fiber PM Er:laser mode locked by a biased NALM is presented. Self-starting fundamental mode-locking operation in single-pulse regime is always observed. The output pulse repetition rate is scaled up nearly three times

*Project supported by the National Natural Science Foundation of China (Grant Nos. 61805282, 11802339, and 11504420), the Opening Foundation of State Key Laboratory of High Performance Computing, China (Grant No. 201601-02), the Open Research Fund of Hunan Provincial Key Laboratory of High Energy Technology, China (Grant No. GNJGJS03), the Opening Foundation of State Key Laboratory of Laser Interaction with Matter, China (Grant No. SKLLIM1702), and the China Postdoctoral Innovation Science Foundation (Grant No. BX20180373).

†Corresponding author. E-mail: tjiang@nudt.edu.cn

© 2019 Chinese Physical Society and IOP Publishing Ltd

from ∼ 46.5 MHz to 121.0328 MHz by cutting pigtails of fiber components. A 12-h test is explored to demonstrate this Er:laser's stability. In contrast to previous researches on mode-locked fiber lasers by NALMs, our system is the most effective ever reported — it utilizes only commercially available all-fiber components and two types of fibers (PM single-mode fiber and PM gain fiber). And what is the most important in all items is that the all-fiber configuration eliminates tedious and elaborates adjustments, and thus enhancing the stability greatly.

2. Experimental setup

Figure 1 shows the schematic diagram of the aforementioned all-fiber PM Er:laser. It was composed of an NALM loop, a linear mirror and a 980-nm laser diode (LD). The NALM loop was fabricated with a 35-cm PM Er:fiber (Liekki, Er80-4/125-HD-PM), a $\pi/2$ nonreciprocal phase shifter, a wavelength division multiplexer (WDM, 980 nm/1550 nm), and a 2× 2 optical coupler (1550 nm, split ratio 30/70). A hybrid mirror-isolator (ISO) component working on the slow axis was used as a linear mirror to provide the output 1. It had an inside dielectric mirror (reflection 90%) and an ISO. The PM Er:fiber was pumped by a 600-mW laser diode (LD) at 980 nm through the WDM. All fiber pigtails of these components were PM passive fibers (PM1550-XP). It was expected that the all-PM fiber configuration would increase the mode-locking stability. The port of the coupler in the outside of the laser cavity was used for pulse train monitoring (output 2). Note that the Er:fiber had a normal group-velocity-dispersion (GVD) of 20.0 ps^2/km and the passive PM1550-XP fibers had a negative GVD of −22 ps^2/km, the intra-cavity pulse would behave in a stretched-pulse regime.

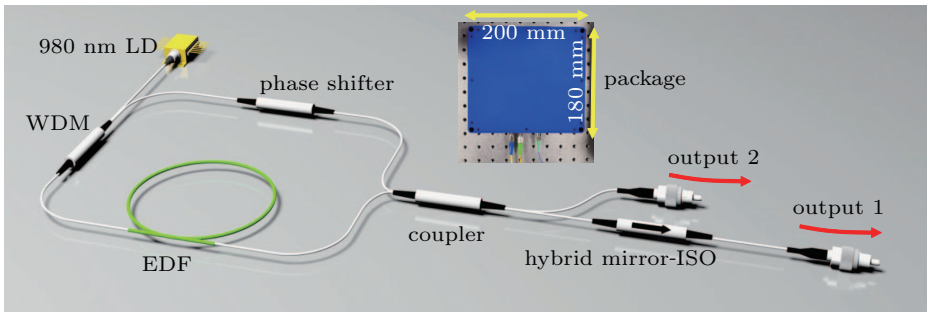


Fig. 1. Schematic diagram of the ultrafast Er:laser. LD: laser diode, WDM: wavelength division multiplexer, ISO: isolator, EDF, Er-doped fiber. Inset shows the package of Er:laser with a size of 180 mm×200 mm×25 mm.

The measurement of the output temporal profile was performed by combining an InGaAs photodetector (with a bandwidth of 12 GHz) with an oscilloscope (with a bandwidth of 1 GHz). A second harmonic generation-based autocorrelator (Femto-chrome, FR-103XL) was used to measure the output pulse width. Other measuring equipment included an optical spectrum analyzer (with a resolution of 0.02 nm), a power meter, a frequency counter (Agilent, 53220 A), and a radio-frequency (RF) spectrum analyzer (with a bandwidth of 1 GHz).

3. Experimental results and discussion

In experiments, a laser cavity is built by directly splicing each of components together without fiber pigtails cut at first. The original laser cavity has a round-trip length ∼ 4.7 m, which corresponds to mode-locking pulses with a repetition rate of ∼ 46.5 MHz. The initial pump power threshold is measured to be ∼ 220 mW. In order to increase the pulse repetition rate, each intra-cavity pigtail is cut into a length of about 10 cm. Figure 2 shows the output pulse repetition rate with respect to the cavity round-trip length in that process. The total cavity dispersion is calculated to be anomalous in a range from −0.076 ps^2 to −0.015 ps^2. The negative cavity dispersion design is important since a stretched-pulse regime demonstrates a low timing jitter.[5]

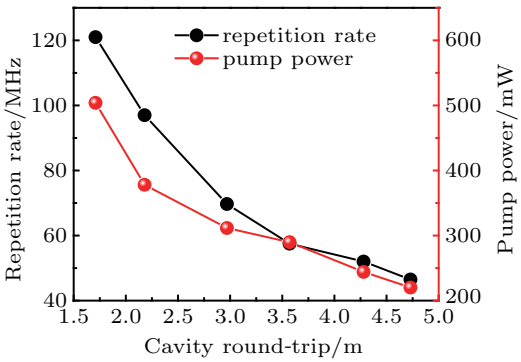


Fig. 2. Variation of pulse repetition rate and pump power threshold with cavity round-trip length.

Fundamental self-starting soliton mode-locking operation is always observed until the output repetition rate reaches to a maximum of 121.0328 MHz. No fiber flapping nor shaking is required. Meanwhile, only single-pulse instead of multiple-pulse is detected. In order to emphasize the key role of phase shifter in the mode-locking operation, we find that no mode lock can be obtained any more if the phase shifter is removed. The reason for this is that the phase shifter contributes to a saturable absorption regime for the intra-cavity pulse. But

when it is removed, the intra-cavity pulse evolves in a reverse saturable absorption regime.[33] Only saturable absorption regime can provide positive feedback for mode-locking operation. Figure 2 also shows the evolution of pump power threshold for the self-starting operation. As can be seen, with the decreasing of the cavity round-trip length, higher pump power is required to implement the mode lock.

To characterize the self-starting process more clearly, the oscilloscope is set to be in the single trigger mode. Then, the 980-nm LD is turned on with the threshold pump power of 504 mW waiting for the onset of modelock. After a very short time, the oscilloscope is triggered and stopped with a record of pulse train. As shown in Fig. 3(a), a typical record waveform can be divided into three regions. At first, an exponential growth is observed due to the fast non-saturable extraction of the stored energy in the Er:fiber. Then after reaching the peak, a slight damping process of pulse amplitudes occurs, which lasts about 40 μs in our experiments. Subsequently, the laser enters into a stable mode-locking state. Figure 3(b) shows the plot of a close look of the steady state. The pulse interval of 8.2 ns is consistent with the cavity round-trip time, showing a single-pulse regime at the fundamental repetition rate once the mode lock is initiated. With repeated measurements, we find that the self-starting process is repeatable and similar results can always be obtained, showing the strict self-starting ability of this laser.

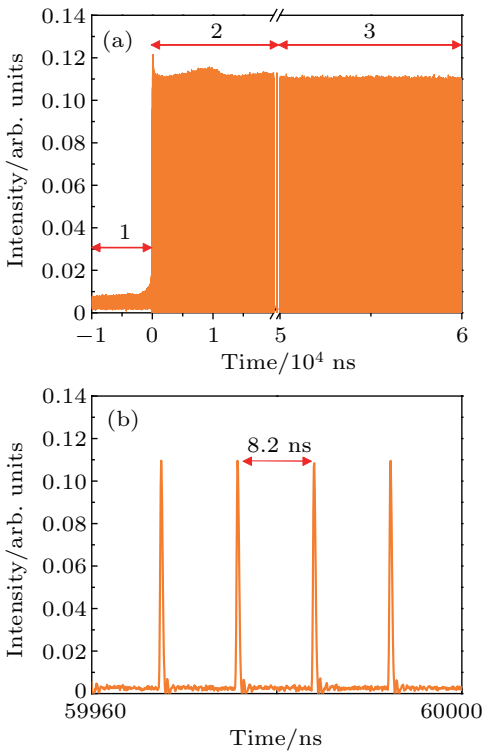


Fig. 3. (a) Build-up process of self-starting mode-locking operation showing: 1 exponential growth, 2 damping state, 3 steady state. (b) A zoom-in plot of the steady state.

Figure 4 shows the optical spectrum, RF spectrum, and intensity autocorrelation of pulses measured at the output 1. As shown in Fig. 4(a), the output laser has a 3-dB spectral bandwidth of 18.7 nm centered at 1571.65 nm, which corresponds to a transform-limited pulse width of ∼ 140 fs. The output can be identified as a soliton pulse from its typical Kelly sidebands on the spectrum although some Kelly peaks are filtered out by the NALM because of their low temporal intensities.

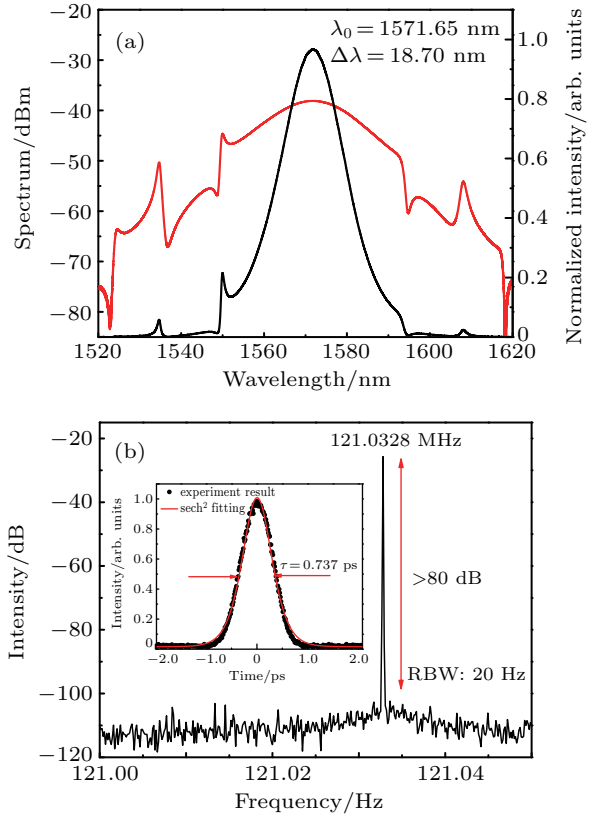


Fig. 4. Output characteristics at 121.0328 MHz. (a) Optical spectrum; (b) first peak of RF spectrum. Inset of panel (b) shows the intensity autocorrelation.

The measured RF spectrum is plotted in Fig. 4(b). It peaks at 121.0328 MHz with a signal to noise ratio (SNR) of > 80 dB, indicating the high stability of soliton lasing in the stretched-pulse regime. The inset of Fig. 4(b) depicts the intensity autocorrelation of the output measured after ∼ 1-m PM1550 fiber. With a secant-curve fitting, the uncompressed pulse width is calculated to be 0.648×0.737 ps $= 477$ fs. Therefore, the output pulse is slightly chirped, which can be de-chirped by using a dispersion compensating fiber.

Moreover, a long-term output test of the Er:laser is conducted. During the test, this laser is placed in an office room where temperature is controlled with an ordinary air conditioner. Figure 5 shows the time evolution of pulse repetition rate, monitored average power (1/4 of the output power) and optical spectrum over 12 h. The long-period fluctuation in Figs. 5(a) and 5(b) is due to temperature variation because the air conditioner works in the energy-saving mode. Although without any active control, the standard deviation of the pulse repetition rate and the average power are calculated to be only 469 Hz and 1.8 pW, respectively, showing that this

free-running ultrafast fiber laser possesses excellent stability. Figure 5(c) shows the laser spectrum evolution recorded in steps of 1 min. Clearly, no shifting of the center wavelength nor any deterioration of the output spectrum shape is observed.

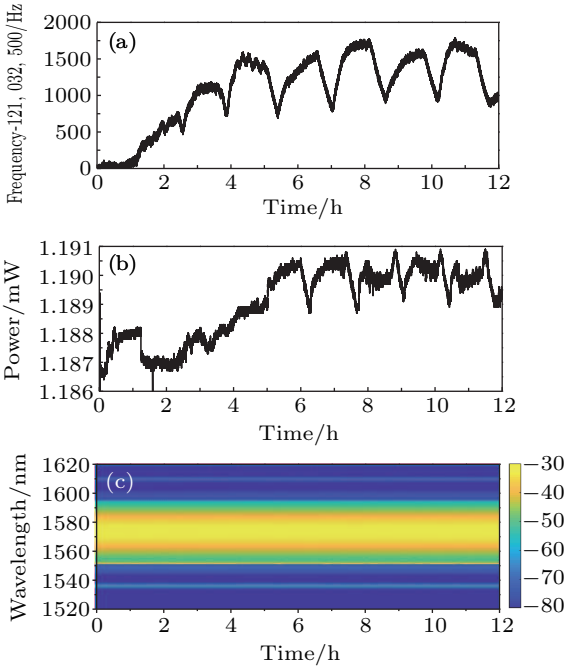


Fig. 5. 12-h measurement of the output show, showing (a) pulse repetition rate, (b) monitored power, (c) optical spectrum, where colorbar represents the spectral intensity in units of dB.

4. Numerical investigation of build-up process

The most popular method used for simulating the propagation of pulse in an optical fiber is the well-known Ginzburg–Landau equation.[37,38] To have a better understanding of the mode-locking principle, the laser configuration used in the experiment is modeled by solving the Ginzburg–Landau equation with an iteration method. The gain saturation coefficient of EDF is changed to realize the mode-locking. All other simulation parameters are in accordance with the experimental setup. The simulation started from an one-photon-per-mode noise signal.

Figure 6 shows the plots of temporal and spectral build-process of mode-locking operation from noise. As shown in Fig. 6(a), stable mode-locking operation in a single-pulse regime is generated successfully after 650 iterations. The corresponding spectral evolution is shown in Fig. 6(b). Obviously, when the output is noise, its spectrum is unstable with narrow spectral bandwidths. Once the output evolves into ultrafast pulse, its spectrum broadens and becomes smooth, which is a typical feature of femtosecond mode-locked pulses.

In order to compare the simulation results with the experimental build-up process, the temporal peak power of output pulse is plotted in Fig. 7. As shown in the figure, three similar states including the exponential growth from noise, the damping state, and steady state are obtained, showing a high degree of consistency between simulations and experiments. What is more, with the numerical investigations, we are also able to uncover the intra-cavity pulse propagation and understand the stretched-pulse mode-locking regime in detail.[39] We also find the mode-locking operation cannot be established if we removed the phase shifter, which is the same as the previous experimental result. In the future, more researches will be conducted to optimize the laser performance. For example, intra-cavity dispersion management is highly desired to realize a low-noise output for optical frequency comb application.

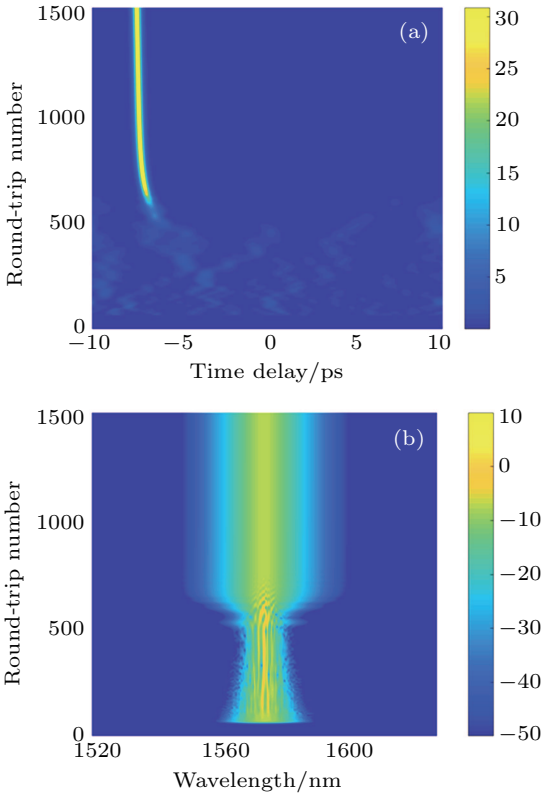


Fig. 6. Dynamic evolution of the build-up process, showing (a) temporal evolution, with colorbar representing output pulse peak power in units of W, and (b) spectral evolution, with colorbar denoting spectral intensity in units of dB.

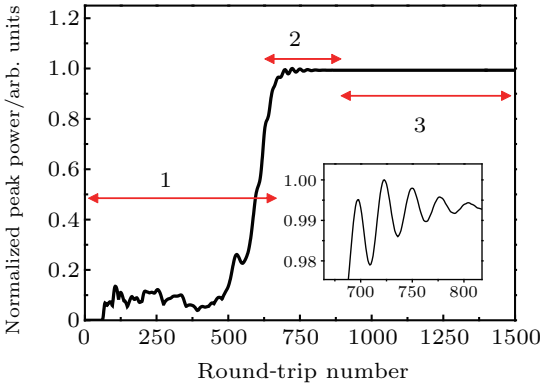


Fig. 7. Peak power evolution of output pulse, showing: 1 exponential growth from noise, 2 damping state, and 3 steady state, with inset showing zoom-in plot of damping state.

5. Conclusions

In conclusion, a compact self-starting all-fiber PM Er:laser with a biased NALM is demonstrated in this work.

Evolution of the output repetition rate with respect to the cavity round-trip length is studied. When the repetition rate is increased to 121.0328 MHz, the self-starting mode-locking build-up process and the stable operation characteristics are further studied. For the first time, the detailed build-up process of Er:laser mode locked by a biased NALM including exponential growth from noise, damping state, and steady state is uncovered both experimentally and numerically. Excellent stability of this self-starting Er:laser is also demonstrated, showing that it is an ideal candidate for compact and robust ultrafast fiber sources.

References

[1] Ngo N Q 2011 *Ultra-fast Fiber Lasers: Principles and Applications with MATLAB Models* (CRC Press)

[2] Dudley J M and Taylor J R 2010 *Supercontinuum generation in optical fibers* (Cambridge University Press)

[3] Yin K, Zhang B, Yao J, Yang L, Chen S and Hou J 2016 *Opt. Lett.* **41** 946

[4] Dvoyrin V and Sorokina I 2014 *Laser Phys. Lett.* **11** 085108

[5] Kim J and Song Y 2016 *Adv. Opt. Photon.* **8** 465

[6] Zhang Y Y, Yan L L, Zhao W Y, Meng S, Fan S T, Zhang L, Guo W G, Zhang S G and Jiang H F 2015 *Chin. Phys. B* **24** 064209

[7] Volpe A, Di Niso F, Gaudiuso C, De Rosa A, Vázquez R M, Ancona A, Lugarà P M and Osellame R 2015 *Opt. Express* **23** 4114

[8] Yin K, Zhang B, Li L, Zhou X, Jiang T and Hou J 2015 *Photon. Res.* **3** 72

[9] Liu W, Pang L, Han H, Tian W, Chen H, Lei M, Yan P and Wei Z 2016 *Sci. Rep.* **5** 19997

[10] Jiang T, Miao R, Zhao J, Xu Z, Zhou T, Wei K, You J, Zheng X, Wang Z and Cheng X A 2019 *Chin. Opt. Lett.* **17** 020005

[11] Wei K, Jiang T, Xu Z J, Zhou J H, You J, Tang Y X, Li H, Chen R Z, Zheng X, Wang S S, Yin K, Wang Z Y, Wang J and Cheng X A 2018 *Laser Photon. Rev.* **12** 1800128

[12] Luo Z C, Liu M, Luo A P and Xu W C 2018 *Chin. Phys. B* **27** 094215

[13] Wang F 2017 *Chin. Phys. B* **26** 034202

[14] Zhang J, Ouyang H, Zheng X, You J, Chen R, Zhou T, Sui Y, Liu Y, Cheng X and Jiang T 2018 *Opt. Lett.* **43** 243

[15] Zhang J, Jiang T, Zhou T, Ouyang H, Zhang C, Xin Z, Wang Z and Cheng X A 2018 *Photon. Res.* **6** C8

[16] Wei K, Xu Z, Chen R, Zheng X, Cheng X and Jiang T 2016 *Opt. Lett.* **41** 3821

[17] Wang J, Yin J, He T and Yan P 2018 *Chin. Phys. B* **27** 084214

[18] Wang J, Jiang Z, Chen H, Li J, Yin J, Wang J, He T, Yan P and Ruan S 2018 *Photon. Res.* **6** 535

[19] Cui Y and Liu X 2019 *Photon. Res.* **7** 423

[20] Yang J M, Yang Q, Liu J, Wang Y G and Tsang Y H 2013 *Chin. Phys. B* **22** 094210

[21] Lee J and Lee J H 2018 *Chin. Phys. B* **27** 094219

[22] Matsas V J, Richardson D J, Newson T P and Payne D N 1993 *Opt. Lett.* **18** 358

[23] Nelson L, Jones D, Tamura K, Haus H and Ippen E 1997 *Appl. Phys. B* **65** 277

[24] Ilday F, Chen J and Kärtner F 2005 *Opt. Express* **13** 2716

[25] Zhang D P J A P S 2012 *Acta Phys. Sin.* **61** 044206 (in Chinese)

[26] Wang J L , Wang X L , He B R , Wang Y G , Zhu J F and Wei Z Y 2015 *Chin. Phys. Lett.* **32** 114202

[27] Ou S M , Liu G Y , Lei H, Zhang Z G and Zhang Q M 2017 *Chin. Phys. Lett.* **34** 074207

[28] Li J, Zhang Z, Sun Z, Luo H, Liu Y, Yan Z, Mou C, Zhang L and Turitsyn S K 2014 *Opt. Express* **22** 7875

[29] Szczepanek J, Kardaś T M, Michalska M, Radzewicz C and Stepanenko Y 2015 *Opt. Lett.* **40** 3500

[30] Guo Z, Hao Q, Yang S, Liu T, Hu H and Zeng H 2017 *IEEE Photon. J.* **9** 1

[31] Aguergaray C, Broderick N G R, Erkintalo M, Chen J S Y and Kruglov V 2012 *Opt. Express* **20** 10545

[32] Wanli Gao W G, Guanyu Liu G L and Zhigang Zhang Z Z 2018 *Chin. Opt. Lett.* **16** 111401

[33] Hänsel W, Hoogl, H, Giunta M, Schmid S, Steinmetz T, Doubek R, Mayer P, Dobner S, Cleff C, Fischer M and Holzwarth R 2017 *Appl. Phys. B* **123** 41

[34] Lezius M, Wilken T, Deutsch C, Giunta M, Mandel O, Thaller A, Schkolnik V, Schiemangk M, Dinkelaker A, Kohfeldt A, Wicht A, Krutzik M, Peters A, Hellmig O, Duncker H, Sengstock K, Windpassinger P, Lampmann K, Hülsing T, Hänsch T W and Holzwarth R 2016 *Optica* **3** 1381

[35] Chen F, Hao Q and Zeng H 2017 *IEEE Photon. Technol. Lett.* **29** 2119

[36] Chang Y, Jiang T, Zhang Z and Wang A 2019 *Chin. Opt. Lett.* **17** 053201

[37] Jeon J, Lee J and Lee J H 2015 *J. Opt. Soc. Am. B* **32** 31

[38] Ma C, Tian X, Gao B and Wu G 2018 *Opt. Commun.* **410** 941

[39] Nishizawa N, Suga H and Yamanaka M 2019 *Opt. Express* **27** 19218